

# A reflectance spectrofluorimeter for real-time spectral diagnosis of disease

Markus G. Müller, Adam Wax, Irene Georgakoudi, Ramachandra R. Dasari, and Michael S. Feld<sup>a)</sup>

*G. R. Harrison Spectroscopy Laboratory, Massachusetts Institute of Technology, Cambridge, Massachusetts 02139*

(Received 2 April 2002; accepted 11 August 2002)

We have developed a portable multiexcitation dye laser system pumped by a 308 nm excimer laser, which can collect fluorescence spectra at 11 excitation wavelengths and a white light reflectance spectrum in less than 200 ms. The system is designed to be used in a hospital setting for *in vivo* tissue analysis based on fluorescence and reflectance spectroscopy. A specially designed optical fiber probe with SMA couplers facilitates easy alignment, important in a clinical setting. An intensified charge coupled device camera provides fast data acquisition with large signal-to-noise (S/N) ratio. The optical and electronic systems are controlled with LABVIEW, which is well suited for real time analysis, to extract diagnostic information. We present typical spectra that demonstrate the large excitation-emission wavelength range over which spectra can be acquired with very good S/N ratios.

© 2002 American Institute of Physics. [DOI: 10.1063/1.1511795]

## I. INTRODUCTION

Fluorescence and reflectance spectroscopy of biological tissue is being widely explored as a clinical tool for cancer and precancer detection.<sup>1-3</sup> Working in a clinical environment imposes significant limitations on design parameters and data acquisition time, and typical instruments for such studies acquire either fluorescence spectra at one or two excitation wavelengths or white light diffuse reflectance, limiting the spectroscopic information obtained. A more complete characterization of the tissue chromophores requires knowledge of both the white light reflectance and the fluorescence excitation-emission matrix (EEM) of the tissue specimen, composed of fluorescence emission spectra acquired at a set of excitation wavelengths. An EEM fully characterizes the fluorescence properties of the sample, providing information about the electronic energy level structure of the fluorophores present. However, in biological tissues, the fluorescence features can be significantly distorted because of tissue absorption and elastic scattering, the same optical properties that determine the reflectance, and special techniques that analyze reflectance and fluorescence together are required to disentangle the absorption, scattering, and intrinsic (undistorted) fluorescence parameters, from which biochemical and morphological changes can be measured and quantified.

Here we describe an instrument, the FastEEM II, developed to study tissue fluorescence and reflectance over the entire UV-visible spectrum *in vivo*, with negligible motion artifacts. The new instrument excites the tissue sample with 11 different laser excitation wavelengths (308–505 nm), resulting in 11 fluorescence spectra, from which an EEM is obtained. At the same time, a white light reflectance spectrum (300–800 nm) is obtained from the same tissue location. The reflectance spectrum is used to acquire information about the absorption and scattering properties of the sample

and, in combination with the fluorescence data, to extract the intrinsic tissue fluorescence.<sup>4</sup> Light is delivered and collected by means of an endoscope-compatible optical fiber probe, and a complete set of data with very good signal-to-noise (S/N) ratio is obtained in less than 200 ms. The instrument is a newly developed version of the FastEEM,<sup>5</sup> and significant modifications have been incorporated in hardware and software to provide faster data acquisition, improved S/N ratio, rapid probe alignment and replacement, and on-line data analysis to extract information about chemical and morphological data in real time. Data can be collected in the presence of operating room or endoscope lights. These features are important for clinical studies on patients undergoing routine diagnostic procedures. The resulting information can help the physician in assessing the presence or absence of disease, and can be used as a real-time guide to biopsy.

Previous researchers have developed EEMs for spectral studies of disease. Zuluaga *et al.* used a filtered xenon arc lamp to obtain 18 fluorescence and 3 reflectance spectra in 4 min.<sup>6</sup> Zuchich *et al.* developed a system that could obtain fluorescence and reflectance spectra of the human lens with a filtered pulsed xenon arc lamp at multiple excitation wavelengths.<sup>7</sup> However, the use of filtered lamps requires a long signal integration time and the absence of a (operating) room and endoscope light, especially in nongated systems.

## II. SYSTEM DESCRIPTION

An instrument for acquisition and analysis of tissue fluorescence and reflectance in a clinical setting must meet several requirements. Native tissue fluorescence (autofluorescence) is weak, thus requiring sensitive detection and strong excitation. Data acquisition must provide a good S/N ratio, yet be rapid enough to avoid motional artifacts and not interfere with the routine clinical procedure. In addition, a wide range of fluorescence excitation and reflectance wavelengths must be available in order to provide complete infor-

<sup>a)</sup>Electronic mail: msfeld@mit.edu

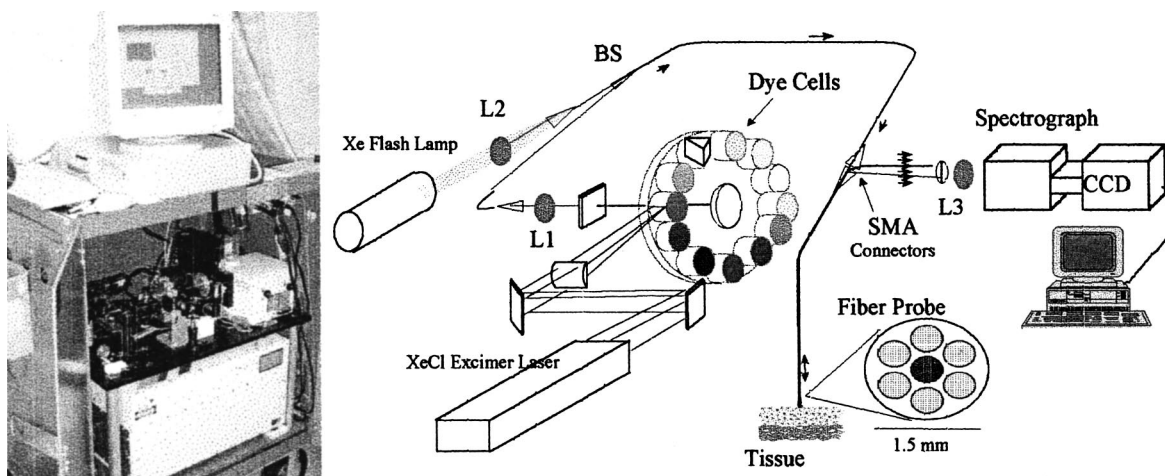


FIG. 1. FastEEM II. Photograph (left panel); and schematic diagram, with excimer laser and flash lamp (right panel).

mation about the optical properties of the tissue sample. Further, the components must be able to be interfaced with rapid on-line data analysis software. Finally, the system must require little maintenance, and must be portable, easy to use, and compact. These design issues were key considerations in the design of FastEEM II.

FastEEM II (Fig. 1) consists of 11 laser excitation sources and a white light xenon flash lamp (Hamamatsu L7684). Ten laser dyes ranging from 342 to 505 nm are pumped by a Lambda Physik Optex XeCl excimer laser (10 mJ 10 ns 308 nm pulses, up to 200 Hz rep rate,  $7.5 \times 4.5 \text{ mm}^2$  beam profile,  $2 \times 1 \text{ mrad}^2$  beam divergence). Laser pump pulses are adjusted to provide 1 to 2 mJ at the dye cells. High laser output energy provides a large dynamic range for pumping the ten dyes, the quantum efficiencies of which vary from 5% to 20% (Table I). The dyes are contained in ten cuvettes mounted on a wheel driven by a motor rotating at approximately 5 Hz. The dye cells are rotated through a laser cavity formed by a planar output mirror and a concave UV-protected aluminum back mirror. When a dye cell is properly positioned, a trigger signal is generated that fires the pump laser (see below). The dye laser output pulse is focused onto a light delivery optical fiber by means of a fused silica condenser lens combination L1 (16 mm focal length). The excimer laser light itself is also used to excite tissue fluorescence.

TABLE I. Excitation wavelengths and dyes and solvents used in the FastEEM. Long pass filters (Schott Glass) are used to cut off the reflected fluorescence excitation light.

Dye	Emission peak (nm)	FWHM (nm)	Solvent	Concentration [mg/20 ml]	Long pass filters
Excimer laser	308				WG 335
PTP	342	5	<i>p</i> -dioxane	10	WG 360
PBD	362	5	<i>p</i> -dioxane	15	GG400
Exalite 384	382	6	<i>p</i> -dioxane	4	GG420
Exalite 398	396	6	<i>p</i> -dioxane	8	GG430
DPS	410	6	<i>p</i> -dioxane	8	GG435
Stilbene 420	425	8	methanol	40	GG455
Coumarin 440	440	10	methanol	36	GG475
Coumarin 460	460	10	methanol	18	GG495
Coumarin 102	480	10	methanol	45	OG 530
Coumarin 500	505	12	methanol	48	OG 550

This is accomplished by means of a right-angle prism and cylindrical lens, positioned in an empty slot on the dye wheel, that redirects the excimer laser beam onto the delivery fiber. The pump laser provides the shortest UV tissue excitation wavelength, which has been chosen to operate in a wavelength range that enables excitation of biologically and diagnostically important fluorophores, such as tryptophan, collagen, and NADH. The white light xenon flash lamp, the source for diffuse reflectance, is focused into a second delivery fiber by means of a fused silica condenser lens combination L2. A filter (custom made by Tacos Inc.) with 50% attenuation in the blue spectral region and 90% transmission otherwise is placed between the flash lamp and L2 to cut off a portion of the strong blue component of the lamp. This provides a more favorable white light spectrum, since the lamp easily saturates the detector in the blue but is quite weak in the red.

The distal portions of the two delivery fibers are fused together to create an optical fiber beam splitter (custom made by Fiberguide Inc.), with the fused fiber carrying light from both excitation sources (loss per source  $\sim 50\%$ ). This arrangement permits us to align the optics associated with each excitation source independently, facilitating alignment. The distal tip is terminated by a SMA connector, which can be quickly and easily mated to the input fiber of the optical fiber probe, which delivers light to the tissue.

The optical fiber probe consists of six collection fibers, 3 m long, surrounding a central delivery fiber (200  $\mu\text{m}$  core diameter, 0.22 numerical aperture). The seven fibers are fused together at the distal tip, creating an optical fused silica shield approximately 1.5 mm in diameter that provides a fixed geometry for light delivery and collection.<sup>8</sup> The shield is beveled and polished at a  $17^\circ$  angle to reduce internal reflections from the boundary between the fused glass tip and tissue. During each measurement the probe tip is brought into gentle contact with the surface of the sample under investigation, and all spectra are collected from the same spot that was excited. The six probe collection fibers are also terminated by SMA connectors. Each of these fibers is then mated to a SMA connector attached to an optical fiber which guides the light through an  $f$ -matched lens to the  $f/4$  spec-

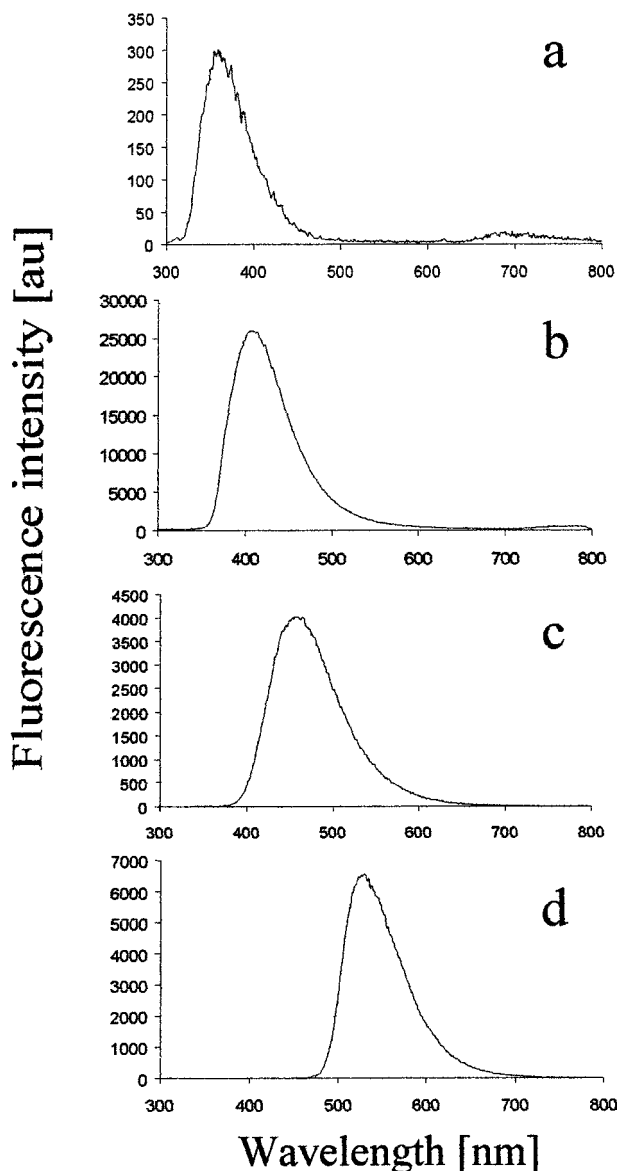


FIG. 2. Fluorescence spectra of endogenous tissue fluorophores. (a) Tryptophan (308 nm excitation); (b) collagen (342 nm excitation); (c) NADH (342 nm excitation); and (d) FAD (460 nm excitation). The different emission line shapes and excitation wavelengths are specific to these fluorophores and can be used to distinguish tissue biochemicals.

trograph (Spectra Pro 150, Acton Research). The spectrograph contains a 300 groove/mm grating blazed at 500 nm, which disperses the light onto an intensified charge coupled device (CCD). The spectral resolution of the system is determined by the spectrograph entrance slit (approximately 0.3 mm), the grating, and the detector binning, and was measured to be approximately 7 nm. This resolution is sufficient for examining the generally broad fluorescence and reflectance spectra of human tissue. The optical fiber arrangement is designed to provide easy maintenance of the system, and the SMA connectors simplify changing optical fiber probes during consecutive clinical procedures. High OH optical fibers with low attenuation are used throughout, and fused silica lenses reduce UV absorption and enable single pulse light collection over a broad wavelength range (fluorescence, 330–700 nm; reflectance, 300–800 nm).

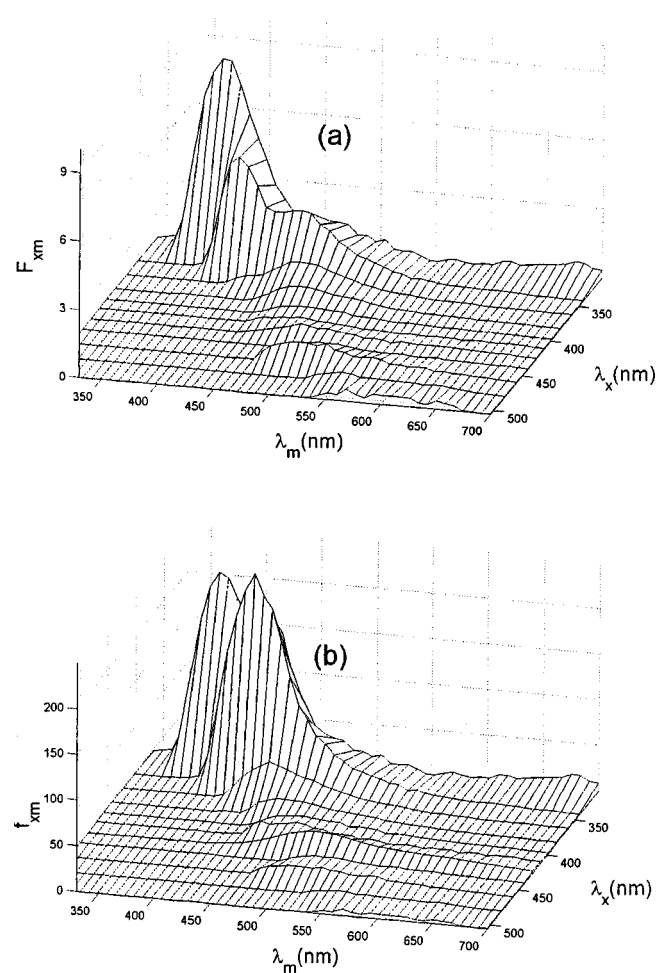


FIG. 3. (a) Tissue fluorescence EEM from a tissue site of a patient undergoing Barrett's esophagus surveillance. The data were obtained in 1 s, and show a very good S/N ratio. (b) Intrinsic fluorescence EEM extracted from (a) using a photon migration model.

The trigger electronics is of our own design. As each dye cell reaches a given position in the laser cavity, a pin attached to the dye wheel generates a trigger signal by passing through an infrared emitter/detector pair. The trigger electronics converts this signal to a 5 V transistor-transistor logic pulse, which is used to trigger the laser or the flash lamp, depending on the position of the wheel. Additionally, the trigger electronics produces a second trigger pulse to open the gate of the ICCD detector. This gate is of variable duration (typically 20  $\mu$ s for tissue studies) and is opened 1  $\mu$ s before the laser fires to ensure that all fluorescence light and reflectance light is collected. This rapid data acquisition minimizes sampling errors due to motion artifacts.

The short read-out time of the ICCD and the short time needed to charge the flash lamp capacitor enables us to collect a full fluorescence EEM (11 wavelengths) and additional white light diffuse reflectance in less than 0.2 s with high S/N ratio. The S/N ratio is further increased by (Peltier) cooling the intensified CCD to  $-20^{\circ}\text{C}$ .

The operation of the system is controlled by a LABVIEW-driven user interface. This software is responsible for control of the laser and ICCD systems. The user interface is an operator-friendly window environment in which the physi-

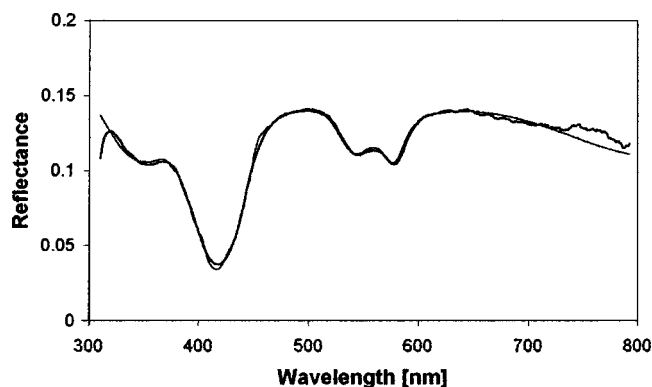


FIG. 4. Diffuse reflectance spectrum (thick line) from the same tissue site as Fig. 3. The DRS model fit (thin line) is also shown.

can display various fluorescence and reflectance spectra, and easily compare data to previous spectra. The software provides simple data processing, as the displayed data can be normalized by various standard measures. In addition, the LABVIEW software provides a means for real-time data analysis by incorporating the ability to process the acquired data using externally called dynamic-link-library (dll) routines written in other programming languages.

### A. System calibration

Thorough calibration of the system is performed prior to data collection. A mercury lamp is used to calibrate the wavelength scale of the CCD detector. A NIST standard tungsten lamp provides spectral response calibration (primarily determined by the spectrograph grating and CCD detector). A spectralon disk (Labsphere) with approximately 20% reflectance is used for white light reflectance calibration to correct for the xenon flash lamp spectral line shape and intensity. Fluorescence intensity correction is achieved using a cuvette with a standardized solution of rhodamine B in ethylene glycol, which allows comparison of tissue fluorescence intensities without day-to-day intensity fluctuations due to small variations in system alignment. Furthermore, by measuring the rhodamine fluorescence response on a well-calibrated spectrofluorimeter at different excitation wavelengths, we calibrate our FastEEM system to account for variations in laser power at the different excitation wavelengths. Finally, a background spectrum for all excitation wavelengths is recorded and subtracted from the patient data to eliminate the offset due to dark counts of the CCD detector and fluorescence and reflectance background created by the optical fiber probe.

The spectral, rhodamine, and background calibration data are stored in the memory of the system and used for automatic calibration and display of the data. Additionally, these files are used in data processing to obtain an on-line diagnosis.

Several concentrations of different fluorophores were measured to determine the sensitivity and response of the system over a large wavelength range.

### B. Real-time data analysis

Software has been developed to perform data analysis in real time. Fluorescence and reflectance spectra have been

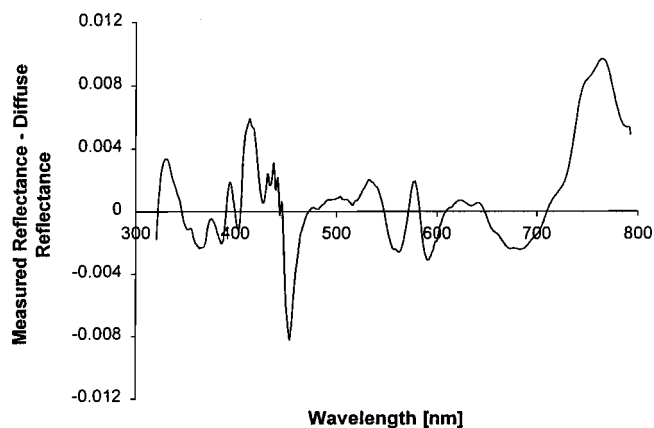


FIG. 5. LSS spectrum from the tissue site of Figs. 3 and 4 obtained by subtracting the model fit of Fig. 4 from the observed diffuse reflectance spectrum.

analyzed using extensive modeling of light-tissue interactions to provide three types of spectroscopic information: intrinsic fluorescence spectroscopy (IFS),<sup>9</sup> diffuse reflectance spectroscopy (DRS),<sup>10</sup> and light scattering spectroscopy (LSS).<sup>11</sup> In the IFS analysis, information from measured fluorescence and reflectance spectra are combined using a photon migration-based model to extract the intrinsic tissue fluorescence, which is free from distortions introduced by tissue scattering and absorption.<sup>4</sup> Intrinsic tissue fluorescence spectra are then decomposed into a linear combination of fluorescence contributions from collagen and NADH, or other diagnostically important chromophores.<sup>3</sup> Thus we extract quantitative biochemical information that can be compared to a specific predetermined threshold to classify the examined tissue site as normal or diseased. The measured reflectance spectra are processed using DRS analysis followed by LSS analysis to extract information from multiply and singly backscattered light. In the DRS step, a light-diffusion theory-based model is used to describe the multiply scattered photons, and thus to extract information about the absorption and reduced scattering coefficients of tissue.<sup>10,12</sup> The spectral features of the reduced scattering coefficient are then used to classify tissue based on preestablished differences in the scattering properties of normal and diseased tissues of the same type. In the LSS step, the spectral features of the multiply scattered light determined from the diffusion model analysis are subtracted from the measured reflectance to provide the spectrum of light that is backscattered from the tissue after undergoing a single scattering event.<sup>11</sup> Analysis of this spectrum yields information on the size distribution and number density of the nuclei of epithelial cells. The values of these parameters are compared to preestablished threshold values to determine whether the light scattering characteristics of the examined tissue sites are consistent with normal or diseased tissue. In the final step of the analysis, information from the IFS, DRS, and LSS analyses is combined to form a consensus diagnosis,<sup>12</sup> which appears in the LABVIEW operator control window.

The entire data analysis process requires up to 10 s for an Intel Celeron processor, and will be significantly faster (~2 s) with a faster computer (Pentium 4).

### III. SYSTEM PERFORMANCE

To illustrate the performance of the instrument, we present clinical spectra from a patient with Barrett's esophagus undergoing standard upper gastrointestinal endoscopic surveillance for dysplasia, a precancerous condition.<sup>13</sup> To acquire these data, the optical fiber probe was passed through the biopsy channel of an endoscope and brought into gentle contact with the tissue. Eleven fluorescence spectra plus one reflectance spectrum with good S/N ratios were obtained in a single 200 ms cycle, and data from five cycles were collected and integrated in less than a second to further improve the S/N ratio to more than 100 to 1. The resulting spectra were calibrated using the procedure discussed above and displayed to the operator in LABVIEW.

FastEEM spectra of common tissue fluorophores, excited at typical wavelengths, are shown in Fig. 2. A tissue fluorescence EEM is shown in Fig. 3(a). Features are present from a number of tissue fluorophores: tryptophan, a common amino acid, which was found to be diagnostic for early cancer detection;<sup>14</sup> the structural protein collagen;<sup>3</sup> NADH, a cellular metabolic marker;<sup>3</sup> and sometimes also porphyrins,<sup>12</sup> associated with the heme cycle and other processes.<sup>15</sup> In addition, features due to FAD, another metabolic marker, may also be present,<sup>1</sup> and features from elastin, not present here, are important in tissues such as arterial.<sup>16</sup> Using the IFS analysis software, the intrinsic fluorescence was extracted [Fig. 3(b)] and a linear combination of contributions from collagen and NADH can be fit to these spectra.<sup>3</sup> The IFS fit coefficients can then be used to make diagnostic predictions.<sup>3</sup>

Figure 4 shows the diffuse reflectance spectrum, calibrated as described above, from the same tissue site. Using the DRS analysis discussed above, the scattering and absorption coefficients of the tissue were extracted. The structure at 420 and 540–580 nm is due to hemoglobin absorption, and the decrease from blue to red is primarily due to elastic scattering from collagen. The value of the scattering coefficient extracted from these data was used as a diagnostic parameter for dysplasia.<sup>12</sup> Additionally by subtracting the model fit from the measured reflectance we are able to extract the LSS spectrum, shown in Fig. 5, which provides information about changes in the size distribution of the epithelial cell nuclei lining the esophagus.<sup>12</sup>

The spectra of Figs. 3–5 were obtained in an ongoing

clinical endoscopy study to diagnose dysplasia in Barrett's esophagus. The results were in good agreement with those obtained by conventional histopathology.

The FastEEM is a fast, easy to use, portable instrument for acquiring tissue fluorescence and reflectance spectra in a fraction of a second with very good S/N ratios. Biochemical and morphological information is obtained through incorporation of software to implement different mathematical models to analyze intrinsic fluorescence, diffuse reflectance, and light scattering data in near real time. Thus the FastEEM can be used to provide important spectral diagnostic information for clinical and laboratory studies.

### ACKNOWLEDGMENT

This research was supported by the National Institute of Health Grant No. P41-RR02594.

- <sup>1</sup>R. Richards-Kortum and E. Sevick-Muraca, *Annu. Rev. Phys. Chem.* **47**, 555 (1996).
- <sup>2</sup>G. A. Wagnières, W. M. Star, and B. C. Wilson, *Photochem. Photobiol.* **68**, 603 (1998).
- <sup>3</sup>I. Georgakoudi, B. Jacobson, M. G. Müller, K. Badizadegan, D. L. Carr-Locke, E. E. Sheets, C. P. Crum, R. Dasari, J. Van Dam, and M. S. Feld, *Cancer Res.* **62**, 682 (2002).
- <sup>4</sup>M. G. Müller, I. Georgakoudi, Q. Zhang, J. Wu, and M. S. Feld, *Appl. Opt.* **40**, 4633 (2001).
- <sup>5</sup>R. A. Zangaro, L. Silveira, Jr., R. Manoharan, G. Zonios, I. Itzkan, R. R. Dasari, J. Van Dam, and M. S. Feld, *Appl. Opt.* **35**, 5211 (1996).
- <sup>6</sup>A. F. Zuluaga, U. Utzinger, A. Durkin, H. Fuchs, A. Gillenwater, R. Jacob, B. Kemp, J. Fan, and R. Richards-Kortum, *Appl. Spectrosc.* **53**, 302 (1999).
- <sup>7</sup>J. A. Zuclich, T. Shimada, T. R. Loree, I. Bigio, K. Strobl, and S. Nie, *Laser Life Sci.* **6**, 39 (1994).
- <sup>8</sup>R. M. Cothren, Jr., G. B. Hayes, J. R. Kramer, B. A. Sacks, C. Kittrell, and M. S. Feld, *Laser Life Sci.* **1**, 1 (1986).
- <sup>9</sup>Q. Zhang, M. G. Müller, J. Wu, and M. S. Feld, *Opt. Lett.* **25**, 1451 (2000).
- <sup>10</sup>G. Zonios, L. T. Perelman, V. Backman, R. Manoharan, M. Fitzmaurice, J. Van Dam, and M. S. Feld, *Appl. Opt.* **38**, 6628 (1999).
- <sup>11</sup>L. T. Perelman *et al.*, *Phys. Rev. Lett.* **80**, 627 (1998).
- <sup>12</sup>I. Georgakoudi *et al.*, *Gastroenterology* **120**, 1620 (2001).
- <sup>13</sup>C. W. Boone, J. W. Bacus, J. V. Bacus, V. E. Steele, and G. J. Kelloff, *Proc. Soc. Exp. Biol. Med.* **216**, 151 (1997).
- <sup>14</sup>M. Anidjar, O. Cussenot, S. Avrillier, D. Etori, M. J. Villette, J. Fiet, P. Teillac, and A. Le Duc, *J. Biomed. Opt.* **1**, 335 (1996).
- <sup>15</sup>J. K. Dhingra, X. Zhang, K. McMillan, S. Kabani, R. Manoharan, I. Itzkan, M. S. Feld, and S. M. Shapshay, *Laryngoscope* **108**, 471 (1998).
- <sup>16</sup>L. I. Laifer, K. M. O'Brien, M. L. Stetz, G. R. Gindi, T. J. Garrand, and L. I. Deckelbaum, *Circulation* **80**, 1893 (1989).